MONTHLY LAND SURFACE TEMPERATURE MAPS OVER EUROPEAN ZONE USING ADVANCED ALONG TRACK SCANNING RADIOMETER DATA FOR 2007.

Galve Joan M.[1], *Coll César*[1] *and Prata Fred*[2]

[1]Department of Earth Physics and Thermodynamics, Faculty of Physics, University of Valencia.
50, Dr. Moliner. 46100 Burjassot, SPAIN.
[2] Department of Climate and Atmosphere, Norwegian Institute for Air Research,
18 Instituttveien, 2015 Kjeller, Norway

Email: joan.galve@uv.es

ABSTRACT

Land Surface Temperature (LST) monthly maps are necessary in climatic studies and remote sensing is a key tool used to obtain these maps. For this reason, we used the LST product of AATSR on board Envisat. This product uses a split-window algorithm which depends on vertical column water vapour content (W) and viewing angle. The algorithm proposed in Galve et al. [1] was also used, which is based on the Coll and Caselles [2] split-window model and depends explicitly on the emissivity and W. This algorithm was tested with concurrent ground measurements in the Valencia validation site, yielding an error of ± 0.5 K. With both algorithms we perform LST maps over Europe with a spatial resolution of 0.05º using the emissivities given in the monthly average of the MODIS MOD11_8D product. Regarding W, we obtain it through the NCEP global Tropospheric Analysis product. In order to evaluate the quality of the maps we resampled these to a 1° pixel size for comparison with the LST from the NCEP Global Tropospheric Analyses product. The most similar algorithm to NCEP LST is Galve et al. [1] with a difference lower than ± 1.2 K. Regarding the maps obtained from the AATSR LST product, the difference was close to ± 1.7 K.

Index Terms— LST, AATSR, monthly maps

1. INTRODUCTION

Land Surface Temperature (LST) monthly maps are needed in order to perform climatological studies. Remote sensing is the most feasible tool for obtaining these maps. Currently, the Envisat / Advanced Along Track Scanning Radiometer (AATSR) does not offer this kind of product. In this work we present LST monthly maps for this sensor over Europe during the 2007.

In order to create these maps we used two methods: One was using the LST product [3] and the other was using the algorithm proposed in Galve et al. [1] algorithm in nadir view. These maps were performed in the zone between the coordinates 72° N - 11° W and 35° N - 42° E with an spatial resolution of 0.05° latitude/longitude.

In order to evaluate these maps, they were resampled to 1° latitude /longitude and compared with the LST yielded by the National Center for Environment Prediction (NCEP) in the global tropospheric analysis product which has a spatial resolution of 1° in latitude/longitude.

In the Methodology section we describe briefly the algorithms used and products needed in order to calculate the LST. Following this section we present an analysis of the assessment of these maps. Finally, conclusions were presented in the last section.

2 METHODOLOGY

The Envisat/AATSR gives measurements in seven bands, where four lie within the visible and near-infrared (0.55 μm, 0.66 μm, 0.87 μm and 1.6 μm) regions and the other three lie within the thermal infrared (3.7 μm, 11 μm and 12 μm). This sensor is able to measure at two different viewing angles: one angle lower than 23.5° with spatial resolution of 1 km^2 and the other between 53° and 55°, with spatial resolution of 3 km^2.

2.1 Algorithms

The LST product of AATSR is based in the split-window method with a set of coefficients that depend on the land use classification. This product depends on vertical column water vapor content and the zenith angle of view [3]. This algorithm uses a linear combination of brightness temperature in the bands at 11 μm and 12 μm (T_{11} and T_{12} respectively) in nadir view. This algorithm can be written as:

$$LST = a_{f,i,w} + b_{f,i}\left(T_{11} - T_{12}\right)^n + \left(b_{f,i} + c_{f,i}\right)\cdot T_{12} \quad (1)$$

where $n=1/\cos(\theta/5)$ and coefficients a, b and c depend on the land surface cover type (i), the fraction of vegetation cover (f), the water vapor content (W) and zenith angle θ.

The algorithm proposed in Galve et al. (ASWn, [1]) was used as an alternative algorithm in this work. This algorithm is based on the Coll and Caselles [2] split-window model and depends explicitly on emissivity (ε, mean emissivity and $\Delta\varepsilon$, spectral emissivity difference) and path column water vapor content ($W/\cos\theta$). The coefficients of the algorithm were obtained from statistical regression of simulations performed with a wide collection of global land radiosoundings (CLAR, [1]). These simulations were performed using viewing angles at nadir, 11.6° and 26.1°. The algorithm can be written as:

$$\begin{aligned} LST_{ASWn} = {} & \\ & T_{11} + 0.024 + 0.782(T_{11} - T_{12}) + 0.302(T_{11} - T_{12})^2 + \\ & (1-\varepsilon)\left(52.57 + 1.13\frac{W}{\cos(\theta)} - 1.023\left(\frac{W}{\cos(\theta)}\right)^2\right) - \Delta\varepsilon\left(79.2 - 11.06\frac{W}{\cos(\theta)}\right) \end{aligned} \quad (2)$$

Currently, there are no emissivity maps for this sensor. To apply the algorithm we used the monthly mean emissivity from the MODIS 8 days product of LST and emissivity (MOD11_8D, [4]) as the bands centered on 11 μm and 12 μm of this sensor are similar to those of AATSR.

An estimation of W is needed in order to apply this algorithm to each pixel in a scene. The NCEP give us global maps of this parameter every 6 hours. In Galve et al. [1] it was demonstrated that the effect of W errors in LST is lower than ± 0.1 K. We used the spatially closest value and interpolated temporally between the earlier and later maps of NCEP.

2.2 LST maps

With both algorithms we perform LST maps over Europe. We used a 0.05º pixel size grid, around 5x5 km^2, from 72° N – 11° W to 35° N – 42° E.

The LST from the AATSR_LST product in each tile was obtained as the mean of the pixels inside of this tile for every day. Later, a monthly mean was obtained through all scenes of the month. In order to solve the statistical errors caused by process errors or undetected clouds, we did not consider values of LST which differ from the mean, in absolute value, by more than three times the standard deviation (σ) of every tile. Seasonal representative months obtained from this algorithm are shown in Figure 1.

In the case of the maps from algorithm ASWn, we started by obtaining the mean of T_{11}, T_{12} and θ in each tile disregarding the values which differ from the mean, in absolute value, by more than 3σ. The LST is calculated for each tile and day using the corresponding emissivity and W. Finally, we obtain the monthly mean of the LST without considering values that differ from the mean by more than $\pm 3\sigma$. Seasonal representative months obtained from this algorithm are shown in Figure 2.

3. ASSESSMENT

The ASWn algorithm was validated with ground measurements yielding errors lower than ±0.5 K ([1]). In Coll et al., ([5-6]) it was demonstrated that the AATSR_LST product overestimated the ground LST by more than 3 K. This error could be due to the spatial resolution of 0.5° latitude/longitude of the land use classification and fractional vegetation cover maps used in this product. The size of this spatial resolution is too large to obtain the LST.

In order to evaluate the quality of the maps, they were compared with the surface temperature (Ts) obtained from the NCEP. These Ts were obtained through the temporal interpolation between the Ts maps given by NCEP before and after the overpass time as in the case of W maps. The LST maps generated were resampled to 1° pixel size (NCEP grid size). We obtained the difference LST - Ts for both algorithms. Figure 3 shows these results for the AATSR_LST case and Figure 4 for the ASWn case.

Figure 5 shows a summary of these results, where the monthly mean difference is shown and the lines represent the mean plus or minus the standard deviation. For the LST maps obtained through the AATSR_LST product, the difference is stable during whole year yielding a mean underestimation in LST of 1.2 K. The highest deviation, -1.9 K, occurs in September and the lowest in April (-0.7 K). The standard deviation of the difference maps were obtained in order to estimate the variability of each map. The mean σ obtained was ± 1.1 K. The mean root mean square error for the whole year is ±1.7 K.

The maps obtained from the ASWn algorithm present better results yielding a mean difference over the whole year of – 0.5 K, the maximum being in February (-1.6 K). From April to September the bias was close to zero (between -0.13 K and 0.14 K). Moreover, the mean σ is ±0.9 K during the year. Finally the mean root mean square error is ± 1.2 K. In the case of ASWn algorithm, it results in a strong seasonal effect, as this algorithm underestimates the LST in the coldest months (October – March) but in the hottest months (April - September) the bias is practically zero. A possible reason for this effect could be that the emissivity given by the MODIS product may not be accurate enough for AATSR in the cold months.

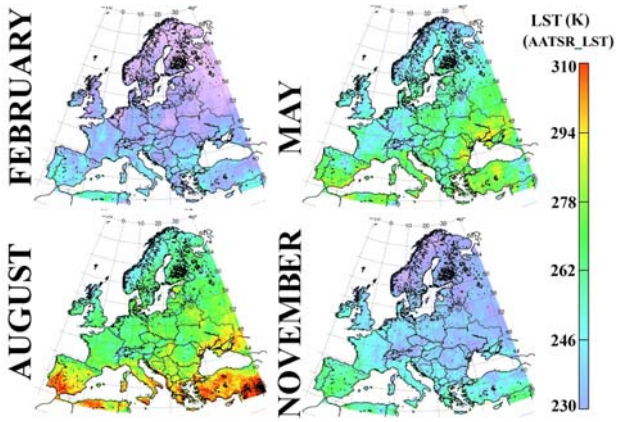

Figure 1.- Monthly LST maps obtained through AATSR_LST product for the seasonal representative months of 2007.

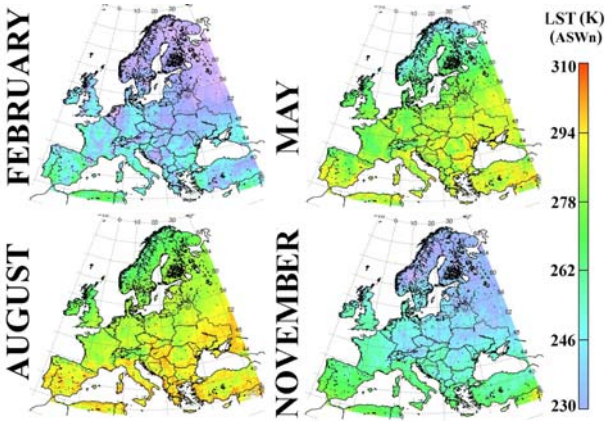

Figure 2.- Monthly LST maps obtained through ASWn algorithm for the seasonal representative months of 2007.

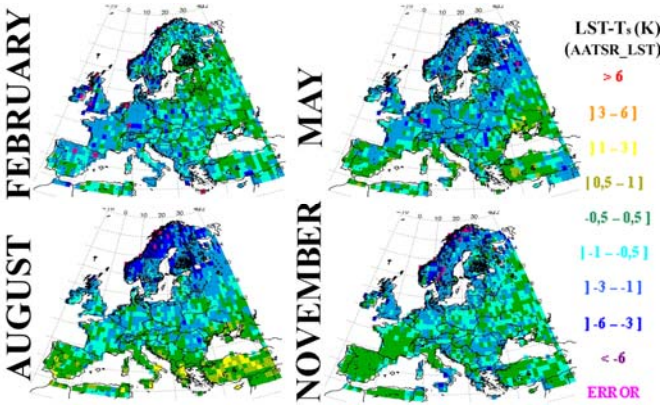

Figure 3.- Monthly LST-Ts maps for the AATSR_LST product case.

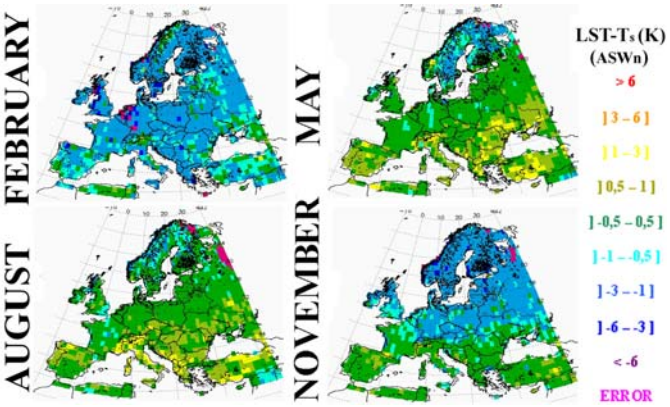

Figure 4.- Monthly LST-Ts maps for the ASWn algorithm case.

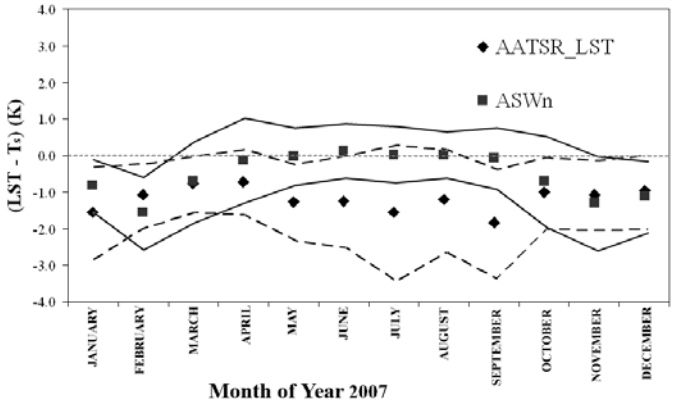

Figure 5.- Monthly mean difference between LST obtained through the algorithms used (AATSR_LST product in diamonds or ASWn algorithm in squares) and the surface temperature (Ts) obtained from the NCEP product. The lines present the standard deviation for each month and algorithm (AATSR_LST in dashed lines and ASWn in solid lines).

This seasonality does not appear in the results for the AATSR_LST case, but the summer months seem to show a larger standard deviation than the other months. We note the fact that the use a spatial resolution of 1° in latitude and longitude reduces the effect of the misclassification that appears in the field campaigns, when we compare regions smaller than 0.5°. Although this resolution reduces the effect of the wrong classification, we can not consider that the error obtained in these maps are absolutely free from this effect, in which case the inaccurate classification could be the reason for the underestimation in the whole year.

4. CONCLUIONS

In this work, we created monthly LST maps from AATSR data during 2007 for use in climatologic studies. These maps were performed over Europe (72°N – 11° W and 35° N – 42° E) with a spatial resolution of 0.05° latitude and longitude. Two different versions of these maps were created according to the algorithm used: in the first, the AATSR LST product was used, and in the second we used the LST algorithm proposed in Galve et al [1]. We compare these maps with the maps of surface temperature obtained from the global tropospheric analysis product from the NCEP in order to assess the quality of these maps.

The results obtained present a mean root mean square error of ±1.7 K which is almost constant over the whole year for the AATSR_LST product. The bias for these maps was close to -1.2 K for the whole year. However, in the case of ASWn the mean root mean square error was ±1.2 K. Despite the AATSR_LST product results, the ASWn algorithm results present a seasonal effect, underestimating by around 1 K in the cold months (October – April) while the bias was close to zero in the warm months (April – September). This seasonal effect should be due to the emissivity maps used for the cold months not being accurate enough.

5. REFERENCES

[1] Galve J.M., Coll, C., Caselles V. & Valor E. “An Atmospheric Radiosounding database for generating Land Surface Temperature Algorithm.” *IEEE Trans. on Geosciences and Remote Sensing*, *46* (5), 1547-1557, (2008).

[2] Coll, C. & Caselles, V. “A split-window algorithm for land surface temperature from Advance Very High Resolution Radiometer data: Validation and algorithm comparison.” *J. Geophys. Res.*, *102*, 16697-16713 (1997).

[3] Prata, A.J. Land surface temperature measurement from space: AATSR algorithm theoretical basis document, technical report, 34 pp., *CSIRO Atm. Res., Aspendale*, Australia (2002).

[4] Z. Wan. MODIS Land Surface Temperature. *Algorithm theoretical basis document* NAS5-31370 (1999).

[5] Coll, C., Caselles, V., Galve, J.M., Valor , E., Niclòs, R., & Sánchez, J.M. “Evaluation of split-window and dual-angle correction methods for land surface temperature retrieval from Envisat/AATSR data”. *J. Geophys. Res., 111*, 12105 doi 10.1029/2005J D006830 (2006).

[6] Coll C, Hook, S.J. & Galve J.M., “Land Surface Temperature from the Advanced Along-Track Scanning Radiometer: Validation over inland waters and vegetated surfaces”. *IEEE Trans. on Geosciences and Remote Sensing*, *47* (1), 350-360, (2009).

ACKNOWLEDGEMENTS

This work was funded by the Ministerio de Educación y Ciencia (Project CGL2007-64666/CLI co-funded with FEDER funds of the European Union, the complementary action CGL2007-29819-E, and the FPI grant of J.M. Galve).